Systematic Assessment of the Influence of Hydrogen Peroxide Dosage on Caffeine Degradation by Photo-Fenton Process

*Evelyn Yamal-Turbay, Moisès Graells, Montserrat Pérez-Moya**

Departament d'Enginyeria Química, Universitat Politècnica de Catalunya.

EUETIB, Comte d'Urgell 187, 08036, Barcelona, Spain.

*Author to whom correspondence should be addressed: Telephone: +34 934137275, Fax: +34 934137401. e-mail: montserrat.perez-moya@upc.edu

Abstract

Caffeine degradation performance via photo-Fenton treatment was investigated under different dosage conditions. Experiments were planned according to a Design of Experiments to characterize hydrogen peroxide dosage protocols. Fenton reagent loads were first determined after a preliminary study. The addition of a fixed hydrogen peroxide load was controlled by an initial load fraction and the span of the continuous flow producing the total load. The experiments were carried out using 12 L solution samples of commercial coffee (300 mg L^{-1}, approximately 17 mg L^{-1} of caffeine). Hence, HPLC data revealed that all treatments completely removed caffeine from samples, while TOC monitoring revealed reductions of up to 70 %. Using reaction conversion as a performance index, the methodological approach presented enabled to compare dosage protocols and to determine those producing enhanced

results. For the particular case addressed, the operation scheme that most increased treatment performance produced a conversion which was 25 % higher than that obtained without dosage.

KEYWORDS. AOPs, photo-Fenton, caffeine, performance assessment, dosage protocol.

1. Introduction

The detection of emerging contaminants[1] in water resources at concentrations[2] below 10 μg L^{-1} has increased the concern on their environmental impact. Remediating wastewaters containing these recalcitrant species requires special treatments, namely Advanced Oxidation Processes (AOPs).[3-5] Particularly, the photo-Fenton option has proved to be low-cost and efficient.[6]

Fenton process has been widely studied over the last three decades, but it was in the 1990's when its use for wastewater treatment boosted research and development. First described by Henry John Hornstman Fenton in the 1890s, the photo-Fenton process involves the *in situ* generation of hydroxyl radicals for the reaction of hydrogen peroxide in the presence of a ferrous salt.[7] Hydroxyl radicals oxidize organic matter, mineralizing it to CO_2, water and inorganic acids. When the reaction mixture is additionally irradiated with UV light, hydroxyl radical production is increased and this photochemical process is known as photo-Fenton process.[8,9] Great efforts have been made in order to propose reaction mechanisms, detect reaction intermediates and understand factors involved in photo-Fenton process.[10,11] However, further work is still required to model the process so that optimal operational conditions can be determined.

One of the most significant factors in photo-Fenton process is the Fenton reagent ratio (Fe^{2+}/H_2O_2).[12] Lots of works have been devoted to determining experimental conditions enhancing treatment performance.[13] Lately, the use of too high Fenton reaction loads were questioned and efforts have been also steered towards reactant reduction[14] with regard to legal limits for iron disposal. Most of this research has mainly considered the batch operation mode, but also the use of an initial load to be progressively consumed along the whole reaction span.

Since hydrogen peroxide has been assumed to undergo diverse parallel competitive reactions of uncertain nature,[13] it seems unrealistic to assume that an initial load of hydrogen peroxide will be under control.

Dosage has been recently described as a relevant factor;[15] the sequential addition of load portions along the reaction time has been reported to improve mineralization,[16] and the study of continuous dosage has lead to promising results.[17,18] Very recently, continuous automatic dosage has been investigated and dosing optimization has been foreseen.[19]

These promising results reveal a great opportunity for improving the efficiency of photo-Fenton processes. A flexible operation may be envisaged thanks to new degrees of freedom upon which practical control recipes could be developed. However, dosage has not been addressed in a systematic way towards this end. There is not only the lack of a convenient model, but also a lack of related experimental data. Therefore, this paper proposes a first step aimed at the experimental characterization of the response of different dosing protocols and the experimental identification of the best dosage tested.

A practical way for parameterizing the dosage is presented and used for planning a set of assays under a Design of Experiments (DOE) scheme. Caffeine is selected for validating this methodological approach to determine the influence of hydrogen peroxide dosage protocol on process efficiency.

Caffeine is almost totally metabolized by the human body. However, rests of beverages containing caffeine are disposed of, and caffeine is detected in low concentrations in sewage treatment plants. Due to its high water solubility and low degradability, caffeine is considered among emerging contaminants.[20,21] Additionally, coffee, the most common mixture containing caffeine, harms the environment due to its opacity and its high biological and chemical oxygen demand, causing eutrophication, blocking light, and affecting photosynthesis.[22,23] Coffee and caffeine deserve more research in order to find better ways to remediate them from wastewaters.

2. Material and methods

Samples to be treated were prepared from instant commercial coffee (Nescafé®) at a concentration of 300 mg L^{-1} in regular water, corresponding to a caffeine concentration around 17 mg L^{-1}. Analytical grade hydrogen peroxide and heptahydrated ferrous sulfate were purchased from Panreac and Merck, respectively, and were used as received. The rest of the chemicals used were, at least, of reagent grade.

Experiments were carried out in a pilot plant using an 8 L reservoir connected to a 2 L tubular photo-reactor provided with a 55 W (maximum power at 254 nm) low pressure mercury lamp PL-L inside of it. pH was maintained at 2.9±0.2 by using a proportional-integral-derivative (PID) controller with HCl and NaOH 1 M as reagents. Temperature, pH, oxidation-reduction potential, dissolved oxygen percentage and conductivity were measured on line.

Initially, 12 L of coffee solution were introduced into the system and were recycled at fixed 11.3 L min^{-1} by a centrifugal pump; next, the Fenton reagent was added during the experiment following the different protocols that are described and discussed in the following sections.

Samples were taken at constant time intervals and, in order to stop the progress of the reaction, they were preserved from light and cooled before being measured.

Total organic carbon (TOC) was determined with a Shimadzu TOC-$V_{CSH/CSN}$ analyzer. Hydrogen peroxide concentration was measured spectrophotometrically after reaction with ammonium metavanadate, following the technique proposed by Nogueira et al.[24] Caffeine concentration was measured via HPLC-UV/DAD using an Agilent 1200 series chromatographic system (Darmstadt, Germany) equipped with an on-line mobile phase degasser, a quaternary pump, a manual injector, a column oven and a UV-diode array detector.

The chromatographic conditions were a 5 µm 4.6x150 mm Zorbax Eclipse XDB-C18 analytical column (Agilent Technologies), maintained at 25 ºC, and the diode array detector set at 274.2 nm. Samples, injected by a manual injector, were eluted by a 70/30 water/acetonitrile mixture (filtered milli

Q grade and J.T. Baker ultragradient HPLC grade, respectively) flowing at 1.5 mL min^{-1}. The retention time of caffeine under these conditions was 1.1 minutes. A five-level calibration curve (range 5.3-84.4 mg L^{-1}) was used for caffeine quantification. It was obtained from working solutions prepared from standard caffeine and injected in the chromatographic system.

Though other experimental conditions such as net irradiative fluxes and wavelengths also influence the degradation performance, they were fixed as pre-established experimental settings. Since the study focuses on the influence of the hydrogen peroxide dosage, Fe(II) load was also fixed after preliminary assays.

3. Preliminary assays and reagent load settings

3.1 Ferrous salt load

The process performance has been proved to be significantly affected not only by the individual concentrations of Fenton reagents, but also by the hydrogen peroxide-to-iron ratio. The selection of this ratio depends on the nature and concentration of the contaminant.[13]

Herney et al.[25] reported a wide range of useful load ratios for the Fenton reagents relative to the degradation of different substances (hydrogen peroxide-to-iron weight ratios from 5:1 to 20:1). Other authors present values in the range from 10:1 to 200:1[26] and even from 100:1 to 1000:1.[13]

The literature indicates the existence of a limiting iron concentration that guarantees the degradation process,[27] conversely, iron excess decreases the effectiveness of the photo-Fenton[28] and Fenton processes.[29]

The work by Tokumura et al.[22] reports on photochemical decolorization of coffee effluents by photo-Fenton process, and investigates the effects of light intensity, initial coffee concentration, and iron and H_2O_2 dose on the color removal of a standard coffee effluent. The initial coffee concentration range was set by Tokumura et al.[22] between 0 and 446 mg L^{-1}, while hydrogen peroxide and iron concentration ranges were set between 0-2400 mg L^{-1} and 0-28 mg L^{-1}, respectively.

According to the results reported by Tokumura et al.,[22] coffee concentration for the standard problem sample was set to 300 mg L^{-1}, and the corresponding load ranges for iron and hydrogen peroxide used were determined in the subsequent set of assays. The first preliminary study was conducted with iron concentrations between 10 and 40 mg L^{-1} and hydrogen peroxide concentration between 1500 and 3000 mg L^{-1}, which implies ratios between 75:1 and 107:1; these data confirmed that total caffeine elimination and TOC reductions between 70 and 80 % are possible via photo-Fenton process. Iron doses of 10, 20 and 40 mg L^{-1} were investigated and very similar TOC reduction profiles where found for the three cases, which suggested the use of the lowest of these doses. Since reduced iron concentration improves economic and environmental performance of the treatment, the iron load was set to 10 mg L^{-1}, which is the legal limit as well.[30]

Similar preliminary conclusions were observed for the H_2O_2 load, and 1500 mg L^{-1} proved to be as efficient as 3000 mg L^{-1}. However, the decision on the H_2O_2 load was made after the complementary assays described in section 3.3.

3.2. **Blank assays**

The next step was to perform a series of blank assays comparing the separate effect of iron, hydrogen peroxide and light (Fig. 1). The blank assays demonstrated that the photo-Fenton process is able to eliminate caffeine and degrade organic matter from the standard samples.

Figure 1. Comparative blank assays of the degradation profile of TOC (solid line) and caffeine (dashed line). Standard sample with $C_{eq,\infty}^{H_2O_2}$ =500 mg L^{-1}

These assays lead to further conclusions:

The sole UV irradiation does not eliminate caffeine, nor reduce TOC.

6

The addition of the oxidant (UV/H_2O_2) produces both the elimination of the caffeine as well as some TOC reduction (clearly, the organic intermediates formed are only partially degraded).

Likewise, the Fenton process is not good enough to mineralize all the organic matter, although it degrades caffeine within a similar treatment time.

The photo-Fenton process not only achieves total caffeine elimination as well, but attains the maximum TOC reduction (around 40%) within the reaction span considered.

3.3. **Stepwise dosage**

Chu et al.[16] investigated the degradation of atrazine by a stepwise Fenton process and showed that Fenton process performance can be significantly improved by splitting the hydrogen peroxide load into several portions dosed along the process. Therefore, in this final set of preliminary assays, different hydrogen peroxide loads and dosage protocols were compared.

The results obtained (Fig. 2) show that the mineralization of the problem samples may be also improved when hydrogen peroxide is dosed at different times and/or quantities along treatment. Furthermore, the same total performance seems to be attainable using reduced hydrogen peroxide loads. In particular, Figure 3 shows that using half of the load (9000 mg) may achieve the same degree of mineralization as using the entire load (18000 mg) if conveniently dosed: 3000 at times 0, 45 and 90 minutes.

The hydrogen peroxide data plotted in Figure 2 correspond to the equivalent concentration ($C_{eq,\infty}^{H_2O_2}$) that would be obtained by having all the additions at time 0. The concept is formalized next in section 4.2. and should not be mistaken for the actual concentration, which needs to be measured each time. For this case, an equivalent initial concentration of 750 mg L^{-1} results from a total amount of 9000 mg (3 x 3000) divided by the total volume of the rector (12 L).

Figure 2. Normalized TOC (solid line) and normalized hydrogen peroxide concentration (dashed line) for the standard sample undergoing three stepwise dosage protocols (gray line). $C_{eq,\infty}^{H_2O_2}$ values are specified in the figure.

Given that, within the 2-hour treatment, up to 75 % TOC reduction may be obtained using 9000 mg (750 mg L^{-1}), a decision was made to set a lower amount as the fixed value upon which the different dosage options were arranged and assessed. Towards this end, 6000 mg (500 mg L^{-1}) of hydrogen peroxide was set as a condition allowing a range of performance outcomes wide enough to be of statistical significance.

Up to this point, reagent total loads have been fixed after preliminary assays (caffeine, 300 mg L^{-1}; iron, 10 mg L^{-1}; hydrogen peroxide, 500 mg L^{-1}). Other structural and operational variables are also fixed. Thus, the remaining degrees of freedom are those related to hydrogen peroxide dosage. At this point, the formalization and parameterization of the hydrogen peroxide dosage is required in order to first determine the governing factors of the process, and next to plan a Design of Experiments (DOE) allowing the identification of the set of operating conditions enhancing process performance.

4. **Experimental design**

Once the loads are fixed (contaminant and reactants), the effect of the way in which one of these fixed amounts is dosed along the time is investigated. The factors governing the dosage need to be first identified and characterized in order to clearly define the problem. The number of factors depends on the degrees of freedom of the dosage protocol adopted: from none, in case the entire load is released at the start, to more degrees of freedom than could be managed in the case a flexible dosing schedule. Furthermore, the option for continuous dosage should be also considered.[17]

Thus, a decision is made for such a trade-off and a three-factor hybrid discrete-continuous dosage protocol is proposed. Given the factors, the assays may be planned (DOE) and executed. Finally, the

definition of a performance measurement is required to quantitatively discern the most promising options.

4.1 Dosage protocol: model and factors

A factor fixed by the previous preliminary study is the total quantity of hydrogen peroxide $Q^{H_2O_2}$ used for each assay. This amount is related to the equivalent mass concentration of hydrogen peroxide $C_{eq,\infty}^{H_2O_2}$, which is defined as the mass concentration that would be obtained in a reactor of volume V_R after the dosage of all the volume v_D^{∞} of hydrogen peroxide of a given purity $P^{H_2O_2}$ (330000 mg L^{-1}), provided the absence of reactions (i.e. just considering the dilution effect):

$$C_{eq,\infty}^{H_2O_2} = \frac{v_D^{\infty} P^{H_2O_2}}{(V_R + v_D^{\infty})} = \frac{Q^{H_2O_2}}{(V_R + v_D^{\infty})} \cong \frac{Q^{H_2O_2}}{V_R} \quad (1)$$

$$v_D^{\infty} = \frac{Q^{H_2O_2}}{P^{H_2O_2}} \quad (2)$$

Being this amount fixed (either $Q^{H_2O_2}, C_{eq,\infty}^{H_2O_2}, v_D^{\infty}$ $C_{eq,\infty}^{H_2O_2} = \frac{v_D^{\infty}\ P^{H_2O_2}}{(V_R + v_D^{\infty})} = \frac{Q^{H_2O_2}}{(V_R + v_D^{\infty})} \cong \frac{Q^{H_2O_2}}{V_R} v_D^{\infty} = \frac{Q^{H_2O_2}}{P^{H_2O_2}}$), the way in which it is dosed along the time is modeled and parameterized in the following way:

$$y(t) = \frac{v_D(t)}{v_D^{\infty}} = \begin{cases} 0 & if\ t < 0 \\ y_0 & if\ 0 \le t < t_{ini} \\ y_0 + \left(\frac{1 - y_0}{\Delta t_{add}}\right)(t - t_{ini}) & if\ t_{ini} \le t < t_{ini} + \Delta t_{add} \\ 1 & if\ t_{ini} + \Delta t_{add} \le t < TS \end{cases} \quad (3)$$

9

where $y(t)$ is the fraction of the total addition that is completed at time t and Δt_{add} is the time increment corresponding to the dosage duration (min).

Therefore, the proposed dosage protocol consists of an initial release y_0 (kick-off) and a constant inflow $m = f(y_0,\Delta t_{add})$ during the time interval $[t_{ini}, t_{ini} + \Delta t_{add})$ and constrained within the treatment span TS. Figure 3 illustrates this dosing procedure and its governing factors.

Figure 3. Definition of the addition protocol. The three independent parameters $(y_0, t_{ini}, \Delta t_{add})$ are highlighted.

4.2 Dosage time interval

The extent of the dosage Δt_{add}, as well as the duration of the entire treatment TS, are next fixed in order to reduce the space of alternatives. Their values were decided according to the results of the preliminary assays and the additional results given by Figure 4.

Figure 4. Comparison of the effect of different dosage span values: Δt_{add}, and kick-off fractions y_0.

Solid lines denote $C^{TOC}(t)$ (■,♦,●) while dashed lines indicate $C^{H_2O_2}(t)$ (□,◊,○). $C_{eq,\infty}^{H_2O_2}$ =500 mg L^{-1}; $C_0^{Fe(II)}$ =10 mg L^{-1}; C_0^{coffee} =300 mg L^{-1}.

Figure 4 illustrates how adding the whole load at the start ($y_0 = 1$) results less efficient than dosing it continuously. The response obtained from $y_0 = 0$ is slower (dC^i/dt), but the progress lasts for longer and further degradation is attained. Regarding TOC reduction, this means that the same load of

hydrogen peroxide is used more efficiently when y_0=0. Namely, part of the load is spent in vain if y_0=1. Actually, competitive hydroxyl reactions have been indicated as the likely cause of such behavior.[13,17]

Conversely, TOC reduction is slightly affected by the extent of the dosage and no significant difference is found between 60 and 120 minutes assays. Accordingly, the values Δt_{add} =60 and TS=120 were set on a practical basis. Finally, it is worth noting that Figure 5 also confirms the fact that, despite the ways in which hydrogen peroxide is supplied and consumed, its disappearance from the system clearly indicates that no further progress can be expected.

4.3 Performance assessment

A quantitative performance index is required (objective function) in order to rank the assays and discriminate the best outcome. This is quite difficult in absolute terms (i.e. economic, environmental, etc.). The achievement of the maximum conversion at the fastest rate (ξ^{max} and k, respectively; eq. 4) was addressed by Pérez-Moya et al.,[31] who suggested a practical multi-objective approach.

$$\frac{dC^{TOC}}{dt} = -k(C_{\infty}^{TOC} - C^{TOC}) \rightarrow \xi = \xi^{\max} e^{-kt} \qquad being \qquad \xi^{\max} = 1 - \frac{C_{\infty}^{TOC}}{C_0^{TOC}} \tag{4}$$

However, parameters such as ξ^{max} and k are measures of a trend, and are thus obtained as a result of a model and the fitting of this model to the experimental data.

Hence, ξ^{max} is not directly measured (neither k), but inferred as the extrapolation of a pattern to infinity. This is feasible even with a very much simplified trend model (eq. 6), but it is impracticable without it. A kinetic model of the reactions under variable dosage needs to contemplate equation 3, but also the “loss” of hydrogen peroxide, for which a single rate parameter is clearly insufficient. This hints again that further detailed modeling is still required.

On the other hand, the performance of the system may be estimated by a direct outcome attained at a certain time. This option is reasonable for data-based modeling, and measuring the contaminant (or TOC) concentration after a given period has been common practice in the AOP literature.

This work takes the outcome ξ after the fixed treatment span *TS* as the performance indicator. It is also assumed that this is a measure of the maximum conversion ξ^{max} attained at infinity, namely:

$$C_{\infty}^{TOC}(\infty) \approx C^{TOC}(TS) \quad (5)$$

This seems a reasonable assumption, since hydrogen peroxide confirmed to have been used up in all the cases. Furthermore, steadiness is also corroborated by the fact that the difference between the last consecutive values of caffeine and TOC concentration was below 5% for all the assays.

4.4 Design of experiments

Once the system and its performance are finally characterized by two factors,

$$\xi^{max} = f(y_0, t_{ini}) \quad (6)$$

a factorial experimental design (2^2) was arranged to quantitatively characterize the effect of hydrogen peroxide dosage on the performance of the treatment under the assumptions up to this point stated.

Two levels (low and high) were considered for t_{ini} and y_0, which were varied in the ranges 0-30 min and 10-30 %, respectively. Three central points for statistical validity and star points at $\pm\sqrt{2}$ were also taken into account. The resulting experimental design is shown in Table 1.

Table 1. Design of experiment variables levels. The resulting dosing slope is also included.

All of the experiments were replicated for statistical validity. Iron (II) and hydrogen peroxide doses of 10 mg L^{-1} and 500 mg L^{-1}, respectively, were set as constant for the design of experiments, which correspond to a 50:1 weight ratio.

$$\frac{C_{eq,\infty}^{H_2O_2}}{C_0^{Fe(II)}} = 50 \quad (7)$$

5. Results and discussion

The summary of the results obtained from the complete set of assays performed is given in Table 2, regarding the performance attained. Assay R corresponds to the reference experiment (no dosage).

Table 2. List of assays carried out: reference (R); design (A to K) and additional (L to N).

Figure 5 shows the evolution of TOC and caffeine concentration for the central experimental conditions (y_0=20 %; t_{ini}=15 min). The average values for the three assays (E, F, G) repeated twice are represented along with the standard deviation in the error bars. These particular conditions attain total caffeine degradation after 45 minutes and reduce TOC by (70.8±3.5) % within *TS*. This performance is comparable to that reported by Tokumura et al.,[22,23] who use higher loads of iron and hydrogen peroxide. Moreover, it is higher than that of the reference assay R obtained with the addition of the entire hydrogen peroxide load at once.

In order to evaluate the influence of investigated factors on ξ^{max}, a statistical analysis was performed by using a commercial statistics software and results demonstrate that y_0 have a significant and positive effect on response (higher initial percentages lead to higher values of ξ^{max}), followed by the interaction between both factors (t_{ini}·y_0).

A similar analysis to identify the factors influencing the time needed to totally degrade caffeine proves that this response mostly depends on initial dosing time (t_{ini}): the earlier the dosing is started, the faster caffeine is degraded. These facts will be demonstrated and discussed ahead.

Figure 5. TOC and caffeine concentration behavior for the central experiment of the design: y_0=20 %; t_{ini}=15 min; $C_{o\ C_0^{Fe(II)}}^{Fe(II)}$ =10 mg L^{-1}, $C_{o\ C_{eq,\infty}^{H_2O_2}}^{H_2O_2}$ =500 mg L^{-1}; $C_{o\ C_0^{Coffee}}^{coffee}$ =300 mg L^{-1}. (◊=TOC

concentration; ♦=caffeine concentration).

In order to help the results discussion from this point on, experiments are named in the figures according to the following nomenclature: "Experiment-code_y_0_t_{ini}".

Table 2 shows the performance improvements (ξ^{max}) achieved by all dosage assays. This behavior can be explained because dosage reduces hydroxyl radical concentration during the first stages of the process, minimizes competitive scavenging reactions, and consequently permits a better use of hydroxyl radicals formed along the reaction time[17].

Regarding the assays whose dosage starts at t_{ini}=15 min (J, E, F, G, K) TOC reduction is clearly higher than the reference experiment (R). Furthermore, the higher y_0, the faster caffeine remediation and higher TOC reduction are achieved. In fact, mineralization around 70 % is possible instead of 60 % observed for the assay R; in particular, for y_0=34.1 % final mineralization (ξ^{max}) increases by 18 %.

Assays A and B in Table 2 allow to discuss the influence of t_{ini} for a fixed y_0 value (10 %). For this low kick-off (few reagent amount) the highest ξ^{max} value is achieved when dosage starts earlier (t_{ini}= 0 min). Moreover, caffeine is also remediated faster in the A assay.

The interaction between both factors (t_{ini}·y_0) is shown in Figure 6, as the statistical analysis performed has already revealed. Both factors are clearly related, assays using low y_0 requires also low t_{ini} in order to obtain high ξ^{max}. In contrast, for higher kick-off, high y_0, a better performance is achieved with higher t_{ini}. However, it is interesting to notice than the influence of t_{ini} diminishes when higher y_0 is dosed. According to caffeine remediation, y_0 is the most influential factor. Faster performance is obtained for higher kick-off values, specifically, caffeine is totally degraded in 25 minutes when y_0=30 %.

Figure 6. TOC and caffeine concentration behavior for different dosage protocols (dashed lines

correspond to caffeine concentration). $C_0^{Fe(II)}$ =10 mg L^{-1}, $C_{eq,\infty}^{H_2O_2}$ =500 mg L^{-1}; C_0^{coffee} =300 mg L^{-1}

Table 2 confirms the importance of the hydrogen peroxide dosage, all the assays obtain higher maximum conversion than the reference assay. An improvement of 15 percentage points of ξ^{max} is achieved with appropriate dosage protocol, equivalent to 25 % global improvement over the reference assay. Thus, the use of the reagent is more efficient and the operation may significantly reduce its cost.

Regarding caffeine, its total remediation is assured during the first minutes of the 120-minute reaction span studied when y_0 is 20 % or higher. In contrast, a lower kick off, y_0, i. e. y_0=10 % reveled not to be enough to obtain a fast caffeine remediation, requiring reaction times around 45-60 minutes.

Additional experiments were performed in order to evaluate the situation outside the boundaries of the design of experiment; Figure 7 shows these results. It is clear that TOC concentration reduction rate is slower when y_0=0 %, but even in this situation higher mineralization is achieved when comparing with the reference assay. In contrast, a higher kick-off than the ones studied, 30 %, has not revealed better performance related to obtaining high maximum conversion (ξ^{max}).

Figure 7. TOC and caffeine concentration behavior for different y_0 at t_{ini}=0min. (dashed lines correspond to caffeine concentration). $C_0^{Fe(II)}$ =10 mg L^{-1}, $C_{eq,\infty}^{H_2O_2}$ =500 mg L^{-1}; C_0^{coffee} =300 mg L^{-1}.

Caffeine is totally degraded in all of the cases, but this goal will be achieved earlier while higher y_0 is provided.

6. Conclusions

The degradation of 12 L solution samples of commercial coffee (300 mg L^{-1}, approximately 17 mg L^{-1} of caffeine) via photo-Fenton treatment ($C_{eq,\infty}^{H_2O_2}$ =500 mg L^{-1} $C_0^{Fe(II)}$ =10 mg L^{-1}) has been studied under different dosage conditions. The study has been carried out using iron loads within the legal limit (10 mg L^{-1}), which is also an advantage in environmental and economic terms.

A hybrid discrete-continuous dosage scheme was proposed using two factors (y_0 and t_{ini}), which was used in an experimental design (2^2) that allowed to obtain the data for quantitatively assessing the influence of Hydrogen Peroxide Dosage on the performance of the photo-Fenton treatment.

The quantitative results showed maximum TOC conversions (ξ^{max}) in the range 60-75% obtained with the same reactant loads but different dosage schemes. The best assay increased treatment performance by 15 percentage points (equivalent to 25 % global improvement over the reference assay: the addition of the load at once (y_0 =1)). The operating conditions of the assay found were y_0=20 % and t_{ini}=36.1 min. Additionally, the DOE has also allowed to provide evidence of the cross-effect between the factors of the dosage protocol.

Regarding caffeine degradation, the HPLC monitoring revealed the complete removal of the caffeine in all the cases, far before the end of the treatment span studied. Moreover, caffeine was degraded more efficiently than previously reported[22] by using lesser amounts of iron and hydrogen peroxide. Qualitative conclusions may be also withdrawn from the degradation time profiles of the caffeine, specially the trade-off between the size of the kick-off (y_0 y_0) and the starting of the continuous dosage (t_{ini} t_{ini}).

This study confirms the importance of the hydrogen peroxide dosage and steps into the opportunity of dosage automation and on-line optimization. Certainly, further work is required in order to fully characterize and exploit more flexible dosage schemes and to understand the effect on the treatment performance. Definitely, this effort includes modeling, definition of the objective function (i.e.

efficiency in terms of cost and time) and the use of additional information, such as on-line measurements of hydrogen peroxide.

Nomenclature

C_0^i : Mass concentration of species i at $t=0$ (mg L^{-1})

$C_{eq,\infty}^{H_2O_2}$: Equivalent mass concentration of hydrogen peroxide (mg L^{-1})

$C^i(t)$: Mass concentration of species i at time t (mg L^{-1})

$P^{H_2O_2}$: Purity of the dosed hydrogen peroxide (mg L^{-1})

$Q^{H_2O_2}$: Total amount of hydrogen peroxide (mg L^{-1})

t_{fin}: Time instant at which the dosage ends (min)

t_{ini} : Time instant at which the dosage starts (min)

Δt_{add} : Time increment corresponding to the dosage duration (min)

TS : Time instant at which the treatment ends; treatment span (min)

$V_D(t)$: Volume of hydrogen peroxide dosed at time t (L)

V_D^∞ : Total volume dosed to the reactor (L)

V_R : Volume of the reactor (L)

y_0: Fraction of the total volume/amount dosed at time $t = 0$ (dimensionless)

$y(t)$: Fraction of the total volume/amount dosed at time t (dimensionless)

Acknowledgments. Financial support received through the research project EHMAN (DPI2009-09386) funded by the European Union (European Regional Development Fund 2007-13) and the Spanish Ministerio de Ciencia e Innovación is fully appreciated. Ms. Yamal wishes to thank Universidad de Carabobo for financial support through professorial grant CD-4352.

Literature cited

(1) Klamerth, N.; Miranda, N.; Malato, S.; Agüera, A.; Fernández-Alba, A.R.; Maldonado, M.I.; Coronado, J.M. Degradation of emerging contaminants at low concentrations in MWTPs effluents with mild solar photo-Fenton and TiO_2. *Catal. Today*. **2009**, *144*, 124.

(2) Becerril, K. Contaminantes emergentes en el agua. *Digital Journal*, **2009**, *10*, 8. [URL: http://www.revista.unam.mx/vol.10/num8/ art54/art54.pdf]

(3) Kaniou, S.; Pitarakis, K.; Barlagianni, I.; Poulios, I. Photocatalytic oxidation of sulfamethazine. *Chemosphere*. **2005**, *60*, 372.

(4) Palominos, R.A.; Mora, A.; Mondaca, M.A.; Pérez-Moya, M.; Mansilla, H.D. Oxolinic acid photo-oxidation using immobilized TiO_2. *J. Hazard. Mater*. **2008**,*158*, 460.

(5) Raja, P.; Bozzi, A.; Jardim, W.F.; Mascolo, G.; Renganathan, R.; Kiwi, J. Reductive/oxidative treatment with superior performance relative to oxidative treatment during the degradation of 4-chlorophenol. *Appl. Catal. B:Environ*. **2005**, *9(3-4)*, 249.

(6) Pérez, M.; Torrades, F.; Domènech, X.; Peral, J. Removal of organic contaminants in paper pulp effluents by AOPs: an economic study. *J. Chem. Technol. Biot*. **2005**, *77(5)*, 525.

(7) Haber, F.; Weiss, J. The catalytic decomposition of hydrogen peroxide by iron salts. *Proc. Roy. Soc. A*. **1934**, *134*, 332.

(8) Pignatello, J.J. Dark and photoassisted Fe^{3+}-catalyzed degradation of chlorophenoxy herbicides by hydrogen peroxide. *Environ. Sci. Technol*. **1992,** *26*, 944.

(9) Safarzadeh-Amiri, A.; Bolton, J.R.; Cater, S.R. The use of iron in advanced oxidation Technologies. *J. Adv. Oxid.Technol.* **1996**, *1*, 18.

(10) Bossmann, S.H.; Oliveros, E.; Göb, S.; Siegwart, S.; Dahlen, E.P.; Payawan, L.; Straub, M.; Wörner, M.; Braun, A.M. New evidence against hydroxyl radicals as reactive intermediates in the thermal and photochemically enhanced Fenton reaction. *J. Phys. Chem*. **1998**, *102*, 5542.

(11) Pignatello, J.J .; Liu, D.; Huston, P. Evidence for an additional oxidant in the photoassisted Fenton reaction. *Environ. Sci. Technol*. **1999**, *33*, 1832.

(12) Gulkaya, I.; Surucu, A.; Dilek, F. Importance of H_2O_2/Fe^{+2} ratio in Fenton's treatment of a carpet dyeing wastewater. *J. Hazard. Mater. B*. **2006,** *136*, 763.

(13) Pignatello, J.J.; Oliveros, E.; MacKay, A. Advanced Oxidation Processes for Organic Contaminant Destruction Based on the Fenton Reaction and Related Chemistry. *Critical Reviews in Environ. Sci. Technol*. **2006,** *36(1)*, 1.

(14) Klamerth, N.; Rizzo, L.; Malato, S.; Maldonado, M.I.; Agüera, A.; Fernández-Alba, A.R. Degradation of emerging contaminants at low concentrations in MWTPs effluents with mild solar photo-Fenton and TiO_2. *Water Res*. **2010**, *44(2)*, 545.

(15) Nilsun, H.I. "Critical" effect of hydrogen peroxide in photochemical dye degradation. *Water Res*. **1999,** *33(4)*,1080.

(16) Chu, W.; Chan, K.H.; Kwan, C.Y.; Choi, K.Y. Degradation of atrazine by modified stepwise-Fenton's processes. *Chemosphere*. **2007,** *67*, 755.

(17) Zazo, J.A.; Casas, J.A.; Mohedano, A.F.; Rodríguez, J.J. Semicontinuous Fenton oxidation of phenol in aqueous solution. A kinetic study. *Water Res*. **2009,** *43*, 4063.

(18) Monteagudo, J.M.; Durán, A.; San Martín, I.; Aguirre, M. Effect of continuous addition of H_2O_2 and air injection on ferrioxalate-assisted solar photo-Fenton degradation of Orange II. *Appl. Catal. B:Environ*. **2009,** *89*, 510.

(19) Prieto-Rodríguez, L.; Oller, I.; Zapata, A.; Agüera, A.; Malato, S. Hydrogen peroxide automatic dosing based on dissolved oxygen concentration during solar photo-Fenton. *Catal. Today*. **2011,** *161*, 247.

(20) Rodríguez-Gil, J.; Catalá, M.; González, S.; Romo, R.; Valcárcel, Y.; Segura, Y.; Molina, R.; Melero, J.; Martínez, F. Heterogeneous photo-Fenton treatment for the reduction of pharmaceutical contamination in Madrid rivers and ecotoxicological evaluation by a miniaturized fern spores bioassay. *Chemosphere*. **2010,** *80*, 381.

(21) Gómez, M.J.; Martínez Bueno, M.J.; Lacorte, S.; Fernández-Alba, A.R.; Agüera, A. Pilot survey monitoring pharmaceuticals and related compounds in a sewage treatment plant located on the Mediterranean coast. *Chemosphere*. **2007,** *66*, 993.

(22) Tokumura, M. ; Ohta, A.; Znad, H.; Kawase, Y. UV light assisted decolorization of dark brown colored coffee effluent by photo-Fenton reaction. *Water Res*. **2006,** *40*, 3775.

(23) Tokumura, M.; Tawfeek, H.; Kawase, Y. Decolorization of dark brown colored coffee effluent by solar photo-Fenton reaction: Effect of solar light dose on decolorization kinetics. *Water Res*. **2008,** *42*, 4665.

(24) Nogueira, R.F.P.; Oliveira, M.C.; Paterlini, W.C. Simple and fast spectrophotometric determination of H_2O_2 in photo-Fenton reactions using metavanadate. *Talanta*. **2005,** *66(1)*, 86.

(25) Herney Ramirez, J.; Costa, C.A.; Madeira, L.M. Experimental design to optimize the degradation of the synthetic dye Orange II using Fenton's reagent. *Catal. Today*. **2005,** *107-108*, 68.

(26) Gernjak, W.; Fuerhacker, M.; Fernández-Ibañez, P.; Blanco, J.; Malato, S. Solar photo-Fenton treatment—Process parameters and process control. *Appl. Catal. B:Environ*. **2006,** *64(1-2)*, 121.

(27) Rossi, I.; Nogueira, R.F.P. Degradation of tetracycline by photo-Fenton process—Solar irradiation and matrix effects. *J. Photoch. Photob. A: Chemistry*. **2007,** *187*, 33.

(28) Pérez-Moya, M.; Graells, M.; del Valle, L.J.; Centelles, E.; Mansilla, H.D. Fenton and photo-Fenton degradation of 2-chlorophenol: Multivariate analysis and toxicity monitoring. *Catal. Today*. **2007,** *124(3-4)*, 163.

(29) Burbano, A.A.; Dionysiou, D.D.; Suidan, M.T. Effect of oxidant-to-substrate ratios on the degradation of MTBE with Fenton reagent. *Water Res*. **2008,** *42*, 3225.

(30) DOGC núm. 3894, DECRET 130/2003, de 13/05/2003, (29.5.2003). (URL: http://www.gencat.cat/diari/3894/03127147.htm, accessed 10/08/2011)

(31) Pérez-Moya, M.; Graells, M.; Mansilla, H.D. A Practical Parametrical Characterization of the Fenton and the Photo-Fenton Sulfamethazine Treatment using Semi-Empirical Modeling. *J. Chem. Technol. Biot*. **2011,** *86*, 826.

List of Figures

Figure 1. Comparative blank assays of the degradation profile of TOC (solid line) and caffeine (dashed line). Standard sample with $C_{eq,\infty}^{H_2O_2}$ =500 mg L^{-1}

Figure 2. Normalized TOC (solid line) and normalized hydrogen peroxide concentration (dashed line) for the standard sample undergoing three stepwise dosage protocols (gray line). $C_{eq,\infty}^{H_2O_2}$ values are specified in the figure.

Figure 3. Definition of the addition protocol. The three independent parameters (y_0, t_{ini}, ΔT_{add}) are highlighted.

Figure 4. Comparison of the effect of different dosage span values: ΔT_{add}, and kick-off fractions Δt_{add} y_0. Solid lines denote $C^{TOC}(t)$ (■,♦,●) while dashed lines indicate $C^{H_2O_2}(t)$ (□,◊,○). $C_{eq,\infty}^{H_2O_2}$ =500 mg L^{-1}; $C_0^{Fe(II)}$ =10 mg L^{-1}; C_0^{coffee} =300 mg L^{-1}.

Figure 5. TOC and caffeine concentration behavior for the central experiment of the design: y_0=20 %; t_{ini}=15 min; $C_{o}^{Fe(II)}$ ($C_{0}^{Fe(II)}$) =10 mg L^{-1}, $C_{eq,\infty}^{H_2O_2}$ ($C_{eq,\infty}^{H_2O_2}$) =500 mg L^{-1}; C_{o}^{coffee} (C_{0}^{Coffee}) =300 mg L^{-1}. (◊=TOC concentration; ♦=caffeine concentration).

Figure 6. TOC and caffeine concentration behavior for different dosage protocols (dashed lines correspond to caffeine concentration). $C_{0}^{Fe(II)}$ ($C_{0}^{Fe(II)}$) =10 mg L^{-1}, $C_{eq,\infty}^{H_2O_2}$ ($C_{eq,\infty}^{H_2O_2}$) = 500 mg L^{-1}; C_{0}^{Coffee} C^{coffee} =300 mg L^{-1}

Figure 7. TOC and caffeine concentration behavior for different y_0 at t_{ini}=0 min. (dashed lines correspond to caffeine concentration). $C_{0}^{Fe(II)}$ ($C_{0}^{Fe(II)}$) =10 mg L^{-1}, $C_{eq,\infty}^{H_2O_2}$ ($C_{eq,\infty}^{H_2O_2}$) =500 mg L^{-1}; C_{0}^{Coffee} C^{coffee} =300 mg L^{-1}.

List of Tables

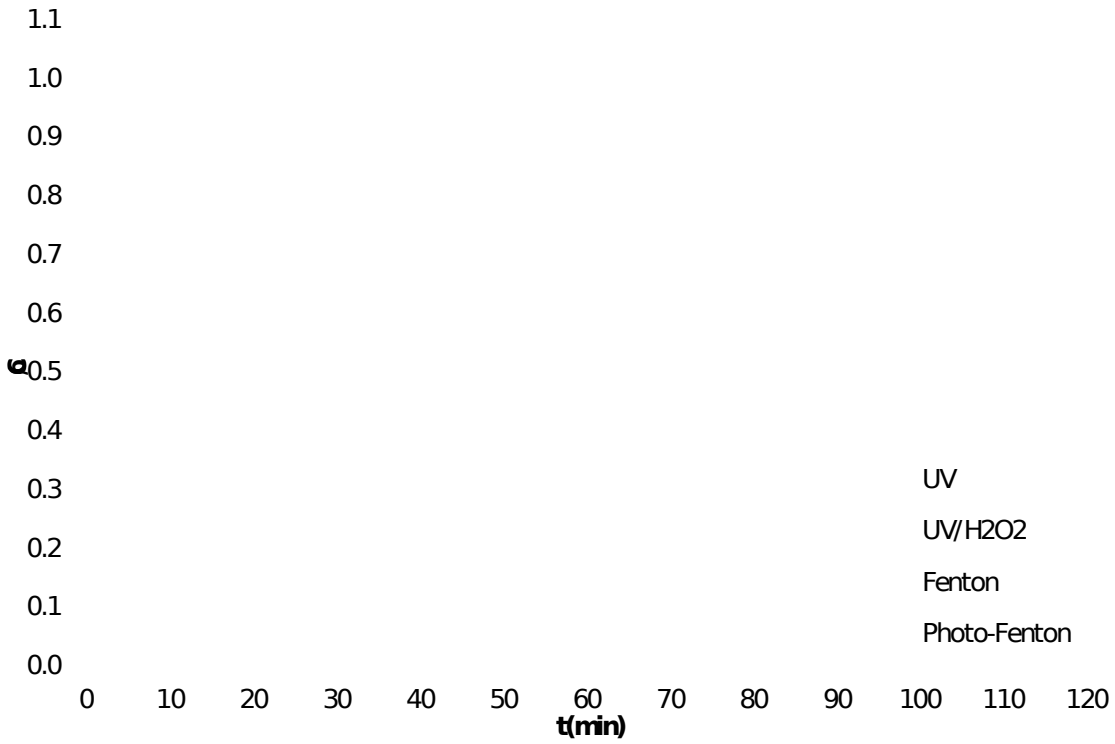

Figure 1. Comparative blank assays of the degradation profile of TOC (solid line) and caffeine (dashed line). Standard sample with $C_{eq,\infty}^{H_2O_2}$ =500 mg L^{-1}

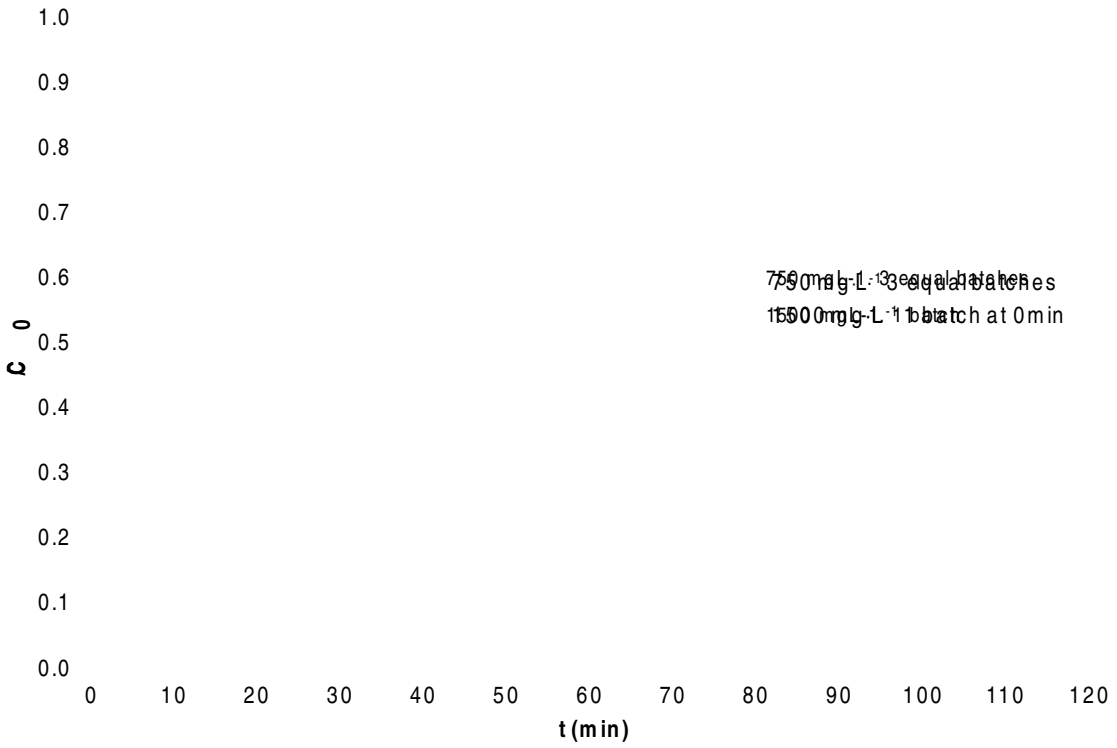

Figure 2. Normalized TOC (solid line) and normalized hydrogen peroxide concentration (dashed line) for the standard sample undergoing three stepwise dosage protocols (gray line). $C_{eq,\infty}^{H_2O_2}$ values are specified in the figure.

434

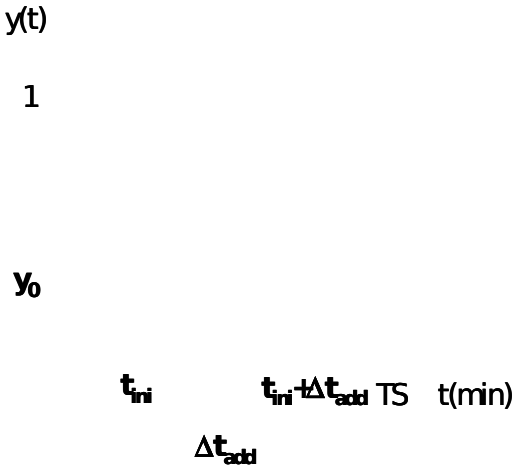

Figure 3. Definition of the addition protocol. The three independent parameters *(y_0, t_{ini}, ΔT_{add})* are highlighted.

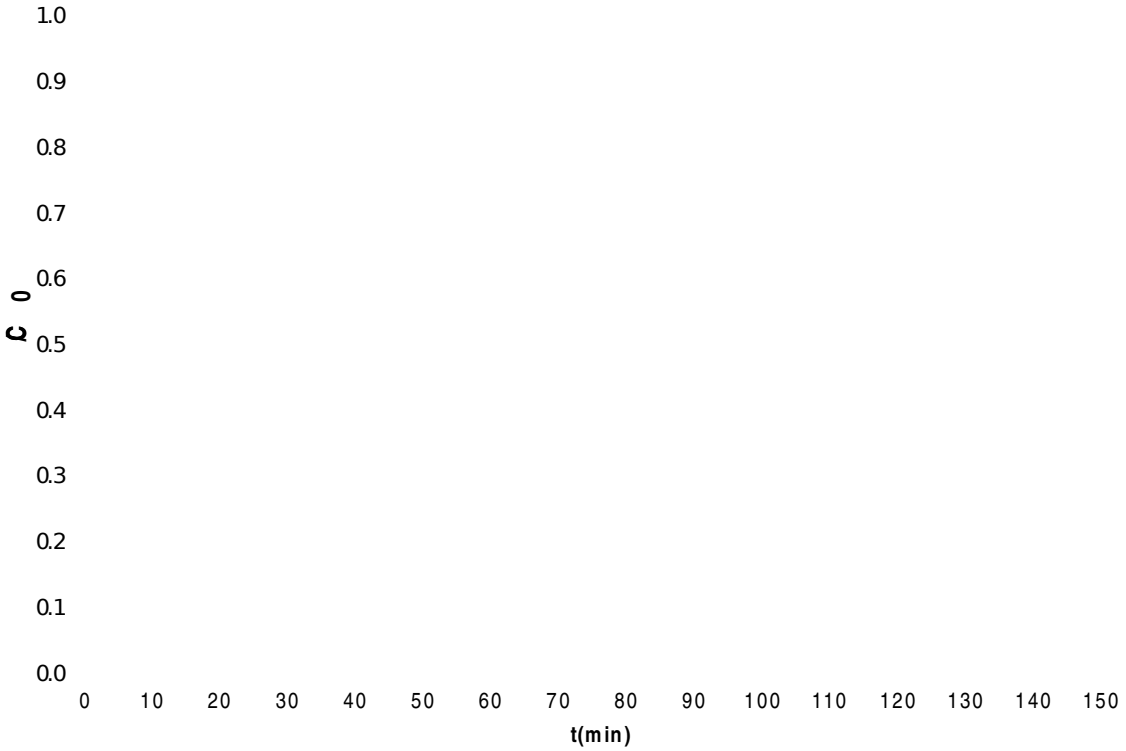

Figure 4. Comparison of the effect of different dosage span values: Δt_{add} ΔT_{add}, and kick-off fractions y_0. Solid lines denote $C^{TOC}(t)$ (■,♦,●) while dashed lines indicate $C^{H_2O_2}(t)$ (□,◊,○). $C_{eq,\infty}^{H_2O_2}$ $C_{eq,\infty}^{H_2O_2}$ =500 mg L^{-1}; $C_0^{Fe(II)}$ $C_0^{Fe(II)}$ =10 mg L^{-1}; C_0^{coffee} C_0^{Coffee} =300 mg L^{-1}.

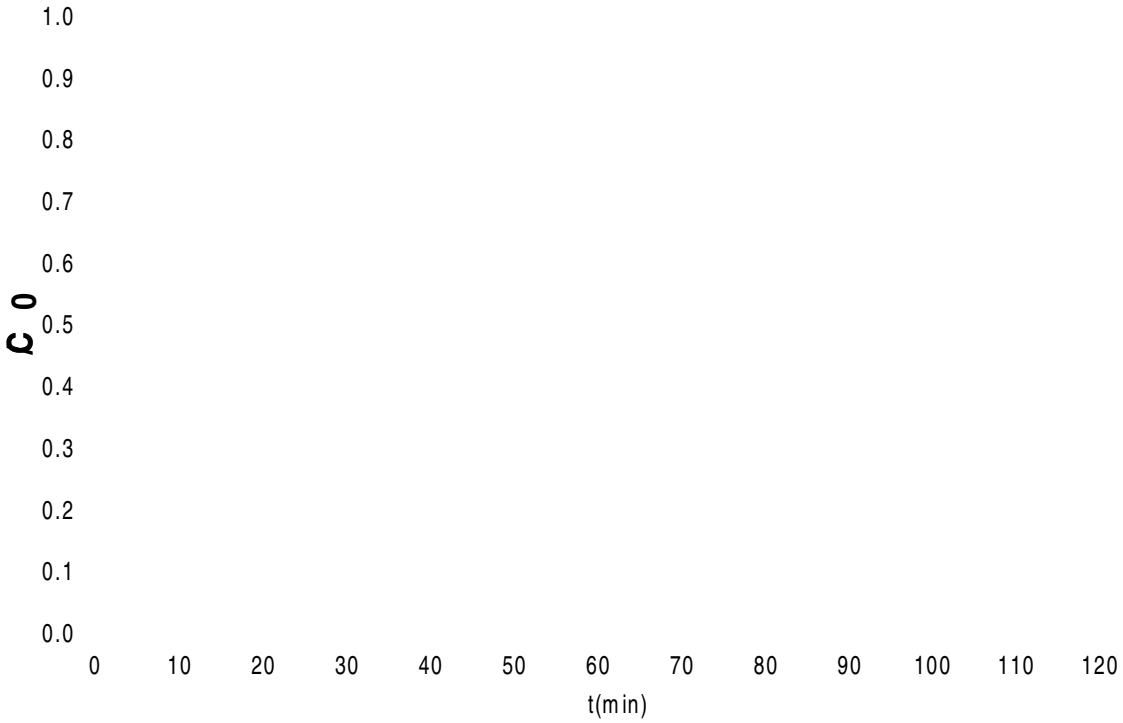

Figure 5. TOC and caffeine concentration behavior for the central experiment of the design: y_0=20%; t_{ini}=15 min; $C_o^{Fe(II)}$ =10 mg L^{-1}, $C_{eq,\infty}^{H_2O_2}$ =500 mg L^{-1}; C_o^{coffee} =300 mg L^{-1}. (◊=TOC concentration; ♦=caffeine concentration).

439

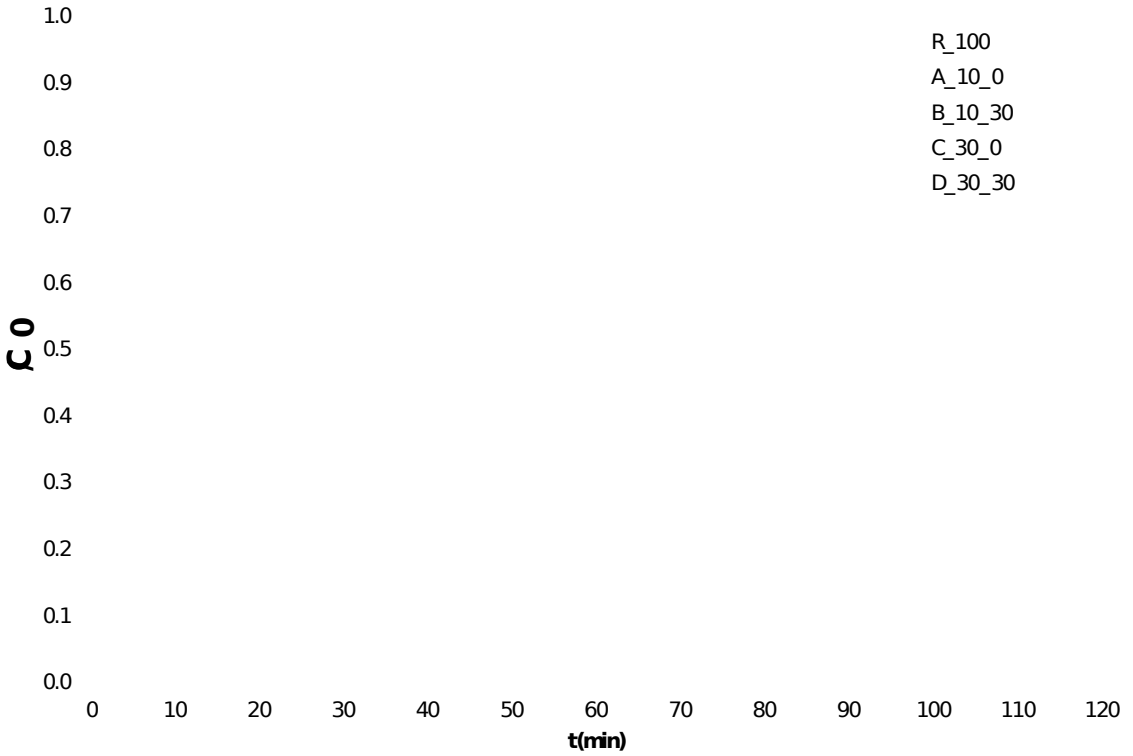

Figure 6. TOC and caffeine concentration behavior for different dosage protocols (dashed lines correspond to caffeine concentration). $C_0^{Fe(II)}$ =10 mg L^{-1}, $C_{eq,\infty}^{H_2O_2}$ =500 mg L^{-1}; C^{coffee} $C_0^{Fe(II)}$ $C_{eq,\infty}^{H_2O_2}$ C_0^{Coffee} =300 mg L^{-1}

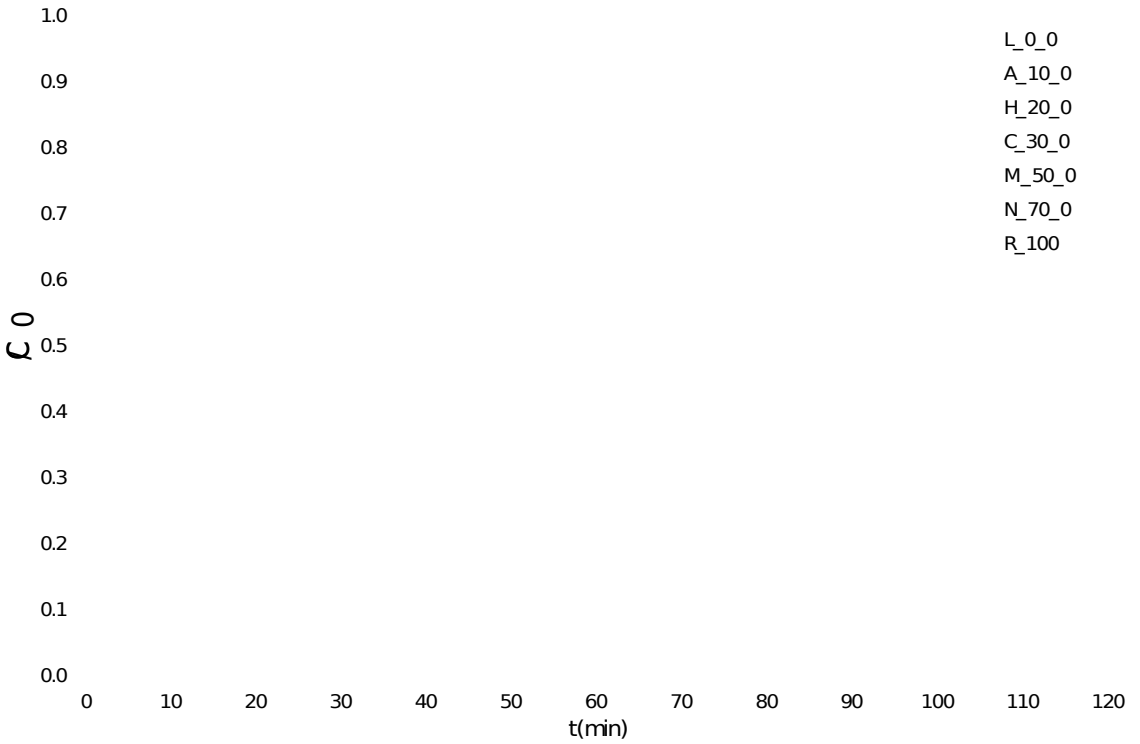

Figure 7. TOC and caffeine concentration behavior for different y_0 at t_{ini}=0min. (dashed lines correspond to caffeine concentration). $C_0^{Fe(II)}$ =10 mg L^{-1}, $C_{eq,\infty}^{H_2O_2}$ =500 mg L^{-1}; C_0^{coffee} =300 mg L^{-1}.

441

Table 1. Design of experiment variables levels. The resulting dosing slope is also included.

Codified values	Variables levels		
	t_{ini} (min)	y_0 (%)	$m = (1 - y_0) / \Delta t_{add}$ (min^{-1})
1	30.0	30.0	1.167
0	15.0	20.0	1.333
-1	0.0	10.0	1.500

Table 2. List of assays carried out.

	Codified values		Actual values		Results	
	t_{ini}	y_0	t_{ini} (min)	y_0 (%)	ξ^{max}	StDev
R	-1	8	0.0	100.0	0.592	0.004
A	-1	-1	0.0	10.0	0.702	0.017
B	1	-1	30.0	10.0	0.650	0.005
C	-1	1	0.0	30.0	0.711	0.018
D	1	1	30.0	30.0	0.720	0.003
E	0	0	15.0	20.0	0.705	0.050
F	0	0	15.0	20.0	0.697	0.037
G	0	0	15.0	20.0	0.721	0.019
H	-1	0	0.0	20.0	0.692	0.059
I	1.414	0	36.2	20.0	0.740	0.035
J	0	-1.414	15.0	5.9	0.674	0.043
K	0	1.414	15.0	34.1	0.715	0.058
L	-1	-2	0.0	0.0	0.689	0.001
M	-1	3	0.0	50.0	0.658	0.006
N	-1	5	0.0	70.0	0.726	0.008